ON THE CORRELATED X-RAY AND OPTICAL EVOLUTION OF SS CYGNI

K.E. McGowan[1], W.C. Priedhorsky[1], S.P. Trudolyubov[1]

mcgowan@lanl.gov

ABSTRACT

We have analyzed the variability and spectral evolution of the prototype dwarf nova system SS Cygni using *RXTE* data and AAVSO observations. A series of pointed *RXTE*/PCA observations allow us to trace the evolution of the X-ray spectrum of SS Cygni in unprecedented detail, while 6 years of optical AAVSO and *RXTE*/ASM light curves show long-term patterns. Employing a technique in which we stack the X-ray flux over multiple outbursts, phased according to the optical light curve, we investigate the outburst morphology. We find that the 3 – 12 keV X-ray flux is suppressed during optical outbursts, a behavior seen previously, but only in a handful of cycles.

The several outbursts of SS Cygni observed with the more sensitive *RXTE*/PCA also show a depression of the X-rays during optical outburst. We quantify the time lags between the optical and X-ray outbursts, and the timescales of the X-ray recovery from outburst. The optical light curve of SS Cygni exhibits brief anomalous outbursts. During these events the hard X-rays and optical flux increase together. The long-term data suggest that the X-rays decline between outburst.

Our results are in general agreement with modified disk instability models (DIM), which invoke a two-component accretion flow consisting of a cool optically thick accretion disk truncated at an inner radius, and a quasi-spherical hot corona-like flow extending to the surface of the white dwarf. We discuss our results in the framework of one such model, involving the evaporation of the inner part of the optically thick accretion disk, proposed by Meyer & Meyer-Hofmeister (1994).

Subject headings: stars: individual (SS Cygni) — novae, cataclysmic variables — X-rays: stars

[1]Los Alamos National Laboratory, MS D436, Los Alamos, NM 87545

1. INTRODUCTION

SS Cygni is a dwarf nova (DN) cataclysmic variable. The main characteristic of DN are outbursts which have recurrence timescales of days to years, and last for days to weeks. Outbursts occur in SS Cygni every ~ 40 d, when the source rises from a quiescent magnitude of $V \sim 12$ to an outburst magnitude of $V \sim 8.5$ (Szkody & Mattei 1984). The outbursts of SS Cygni exhibit a bi-modal distribution, with wide and narrow outbursts that last ~ 20 and ~ 12 d, respectively (Szkody & Mattei 1984).

SS Cygni was first detected in X-rays by Rappaport et al. (1974). The main site of X-ray emission in DN is believed to be the boundary layer between the white dwarf and the accretion disk. Accretion material in the innermost orbit of the disk is decelerated in the thin boundary layer before coming to rest on the surface of the white dwarf. During this process the material should release $\sim$ half of its accretion luminosity.

SS Cygni shows both hard and soft X-ray spectral components (Córdova et al. 1980). The two spectral components are usually attributed to different states of the boundary layer flow, which depend on $\dot{M}$ (Pringle & Savonije 1979). For $\dot{M} \ll \dot{M}_{\rm crit}$, $\dot{M}_{\rm crit} \sim 10^{16}$ g s^{-1}, the heated gas expands adiabatically and forms a hot ($T \sim 10^8$ K) corona which cools by thermal bremsstrahlung, radiating a hard spectrum. For $\dot{M} \gg \dot{M}_{\rm crit}$ the heated gas cools without expanding out of the optically thick boundary layers, giving rise to an approximate blackbody spectrum (at $T \sim 10^5$ K). During this high-accretion state, tenuous regions of the boundary layer flow, above and below the center plane, remain in the hot, optically thin state, yielding a residual hard component.

Comparison of X-ray data from *EXOSAT* with the optical light curve of SS Cygni by Jones & Watson (1992) confirmed this X-ray behavior. In quiescence, the hard component is strong. The outburst is first seen in the optical band. After a short delay the hard X-ray component flares, then declines to a level below that of quiescence. The ultrasoft X-ray outburst begins as the hard X-ray flare ends. The ultrasoft X-ray emission tracks the optical emission closely during the peak of the optical burst, but the ultrasoft X-rays decline to quiescence more quickly. Once they start to decline, the hard X-ray component increases again, to a level brighter than quiescence, then declines more slowly than the optical in the final decline. Studies of detailed *RXTE*/PCA observations of single outbursts of SS Cygni exhibit this X-ray/optical behavior (Wheatley, Mauche & Mattei 2000; Priedhorsky, Trudolyubov & McGowan 2002; McGowan, Priedhorsky & Trudolyubov 2002; Wheatley, Mauche & Mattei 2003).

We analyze several outbursts of SS Cygni from archival data, to investigate the optical and X-ray evolution of the source. In particular, we want to confirm the optical/X-ray

outburst phenomenology found in previous works, which were based on studies of only a few outbursts.

2. OBSERVATIONS AND DATA ANALYSIS

Its brightness and frequent outbursts makes SS Cygni an ideal candidate for observations by amateur astronomers. Since its discovery in 1896, SS Cygni has been monitored by the American Association of Variable Star Observers (AAVSO*). We have obtained the 1996–2001 light curve of SS Cygni from the AAVSO.

We have also obtained the X-ray light curve of SS Cygni from the All Sky Monitor (ASM; Doty 1988; Levine et al. 1996) that is onboard the *Rossi X-ray Timing Explorer (RXTE)* satellite† (Bradt, Rothschild & Swank 1993). The data contained in the archive includes background subtraction. The ASM has three X-ray channels spanning $1.3-12.2$ keV‡, from which we derive $1.3-3.0$ keV (BAND1) and $3.0-12.2$ keV (BAND2) fluxes for our analysis. While the ASM is small, with a 90 cm^2 effective area, it is persistent in its coverage.

We also use the much more sensitive, but sporadic, pointed observations taken by the Proportional Counter Array (PCA; Jahoda et al. 1996) instrument on *RXTE* in the $3-20$ keV band. For our analysis we used publicly available *RXTE*/PCA data collected during $1996-2000$ (a total of 262, observations $\sim 1000-20000$ s duration). The observation log for the data used in our analysis is shown in Table 1.

The PCA data were reduced with the standard *RXTE* FTOOLS package, version 5.2. We used PCA data collected in the $3-20$ keV energy range for the spectral analysis. The PCA response matrices for individual observations were constructed using the *pcarmf* task and the background estimation was performed by applying *very large events* (VLE) or *faint* source models, depending on the level of the source flux §. The standard dead-time correction procedure was applied to the PCA data. In order to account for the uncertainties of the response matrix, a 0.5% systematic error was added in quadrature to the statistical error for each PCA energy channel.

We generated energy spectra of SS Cygni averaging the data over whole individual

*http://www.aavso.org

†http://xte.mit.edu

‡ftp://legacy.gsfc.nasa.gov

§See http://heasarc.gsfc.nasa.gov/docs/xte/recipes/pcabackest.html

observations using the *Standard 2* mode data (binned data; 129-channel spectra accumulated every 16 s). For the temporal analysis of SS Cygni we used the PCA data in *Standard 2* and *Good Xenon* modes (unbinned data; time-stamped events with 256-channel resolution).

3. COMPARISON OF AAVSO DATA AND ASM DATA

The contemporaneous AAVSO and ASM data cover the period from 1996 January 4 to 2001 August 30. The data are shown in Fig. 1; while the optical outbursts are obvious, it is difficult to see individual outbursts in the X-rays.

In order to investigate the optical and X-ray variability we have adopted a stacking technique to average the optical and X-ray data and improve signal to noise. The analysis of the outburst and quiescent (inter-outburst) data are presented in the following sections.

3.1. Outburst

We separate the optical data into wide (Fig. 1, e.g. JD 2450320), narrow (Fig. 1, e.g. JD 2450370), and anomalous or mini outbursts (Fig. 1, e.g. JD 2451050). In our data we find 22 wide, 27 narrow and 7 anomalous outbursts. For rescaling purposes we define start (T_{start}) and end points (T_{end}) to occur at $V = 10.5$ for the wide and narrow optical outbursts, and at $V = 11.7$ for the anomalous outbursts. By calculating the average duration of the wide, narrow, and anomalous outbursts we determine a characteristic length ΔT for the three different outbursts (ΔT = 16 d for the wide, 9 d for the narrow and 3 d for the anomalous outbursts). To ensure we do not ignore any data which may be part of an outburst we include $\sim$ 30 d prior to T_{start} and $\sim$ 40 d after T_{start} in each cut of data for the wide and narrow outbursts, and $\sim$ 5 d before and $\sim$ 10 d after T_{start} for the anomalous outbursts. Using the start and end times of the sections of optical data, we separate the BAND1 ($1.3 - 3.0$ keV) and BAND2 ($3.0 - 12.2$ keV) X-ray data. The optical and X-ray data are rescaled on the characteristic outburst timescales such that $T_0 = T_{start}$ and $T_{\Delta T} = T_{end}$. We can then calculate the average time history for each type of outburst, in the optical, BAND1 and BAND2 X-rays, by stacking and averaging the rescaled data (Fig. 2).

For both the wide and narrow outbursts (Fig. 2, *left and middle panels*), the BAND2 X-rays ($3 - 12.2$ keV) are anti-correlated with the optical flux, i.e. *the* BAND2 *X-ray flux falls when the optical flux rises during outburst*. This is consistent with previous reports that the hard X-rays are suppressed during optical outburst (Jones & Watson 1992; Priedhorsky et al. 2002; McGowan et al. 2002; Wheatley et al. 2003). We have confirmed that this behavior holds

over a large ensemble of outbursts. The previously-reported X-ray maximum at the decline of an outburst is also visible. The BAND2 X-rays for the narrow outburst shows an increase in flux which could be associated with the previously-reported X-ray maximum at the beginning of the optical outburst (Fig. 2, *middle panel*). However, as this is based on only one point, and a similar behavior is not seen in the wide outburst, this result is inconclusive. The averaged anomalous outbursts (Fig. 2, *right panel*) suggest a positive correlation between the optical and BAND2 X-ray flux.

3.2. Quiescence

We studied the optical and X-ray correlation during quiescence using a similar method as for the outburst data. We use the start and end times of the optical outbursts determined above to separate the inter-outburst data. The inter-outburst was therefore the interval between the $V = 10.5$ crossing on the decline from outburst, and the $V = 10.5$ crossing on the rise to outburst. We note that this is an arbitrary definition of quiescence, which we use only for our stacking analysis. We removed all data from times of anomalous outburst. We calculate the average duration of quiescence, and define a characteristic length for the quiescent interval of 38 d which we used to rescale the data. The optical, BAND1 and BAND2 X-ray data are then averaged by stacking all the quiescent intervals (Fig. 3).

A linear fit including a decline to the inter-outburst $1.3-12.2$ keV X-ray flux of SS Cygni results in a χ^2 of 36.8 for 29 d.o.f. We chose the interval from rescaled days 5 to 36 as the largest span that is clearly free from the optical outburst. During this interval the flux seems to fade, with a decline significant at the 3.6-sigma level. The error bars on the ASM X-ray fluxes reflect all currently known systematic effects. The best linear fit to the $1.3-12.2$ keV X-ray flux between rescaled days 5 and 36 declines at the rate of 1.3% per scaled day, with a decrease of $\sim 40\%$ over the day 5 – day 36 interval (see Fig. 3, *fourth panel*). In other words, the flux between days 5 and 36 was fit by a mean flux of 0.354 counts s^{-1} and a slope of -5.7×10^{-3} counts s^{-1} day^{-1}, with an error in the slope of $\pm 1.6 \times 10^{-3}$ counts s^{-1} day^{-1}, based on an increase in the χ^2 of 1 for one interesting parameter.

3.2.1. Folding on the Orbital Period

To test for a modulation at the orbital period, we combined the BAND1 and BAND2 X-ray data from the same quiescent intervals. We folded the $1.3-12.2$ keV data on $P_{orb} = 0.2751297$ d using $T_0 =$ HJD 2447403.6295, where T_0 corresponds to the time of inferior

conjunction, i.e. the time of zero velocity of the absorption line star (Friend et al. 1990). The resulting light curve is shown in Fig. 4.

We fit the data with a constant linear fit and a sinusoid. The best linear fit results in $\chi^2 = 7.1$ for 19 d.o.f., the best-fit sinusoid gives $\chi^2 = 5.4$ for 16 d.o.f. The semi-amplitude of the sinusoid is 0.024 counts which corresponds to a 7% modulation. While the sinusoid gives a better fit to the data, employing the F-test we find a probability of 78%. This indicates that the variation is random, thereby failing to rule out a constant flux.

4. COMPARISON OF SHORT-TERM OPTICAL AND X-RAY TIME HISTORIES

4.1. Light curve phenomenology. Correlated hard X-ray and optical evolution.

In five years, six optical outbursts of SS Cygni were covered with *RXTE*/PCA pointed observations. Two of the outbursts were poorly sampled, therefore we present results from only four of the outbursts here. In spite of the differences in the duration of the four outbursts, the morphology of the hard X-ray evolution ($3 - 20$ keV) is essentially the same in each (Fig. 5, *upper and middle panels*). Unlike the soft X-ray emission below ~ 1 keV (Jones & Watson 1992), the hard X-ray emission of SS Cygni shows a general anticorrelation with optical flux, except for "brief" X-ray/optical outbursts ('spikes'). The positions of the *spikes*, which last for < 2 d, are marked in Fig. 5 (*right panel*) at MJDs 51610, 51622, 51644 and 51680. The rise of the optical outburst coincides with a short *spike* in the hard X-rays: the flux increases by several times, then fades, all in $\lesssim 1$ d. At the maximum of the optical outburst, the hard X-ray flux is at its lowest. The decline of the optical outburst corresponds to a gradual increase of the hard X-ray flux, followed by a brief $2 - 4$ d maximum. Periods of optical quiescence are generally characterized by a relatively high level of hard X-ray flux. Rare anomalous optical outbursts are accompanied by short X-ray *spikes* (i.e. MJDs 51610 and 51644 in Fig. 5, *right panel*).

We studied the characteristic timescales of the hard X-ray luminosity transitions. The average duration of the X-ray *spike* coincident with an anomalous optical outburst is $\lesssim 2$ d, with a nearly symmetrical time history. Exponential fits to the rising/decaying parts of the X-ray *spikes* (MJDs 51610 and 51644) give an e-folding time of ~ 0.5 d (Fig. 5).

The X-ray *spikes* corresponding to the beginning of the optical outburst have a shorter duration of $\lesssim 1$ d. The observations of 1996 October 9–11 allow a detailed study of the source evolution during such a *spike* (Fig. 5, *left panel*). The light curve of SS Cygni during the *spike*, based on four consecutive PCA observations (Wheatley et al. 2000; Wheatley et al. 2003),

is shown in Fig. 6.

The *spike* has an asymmetric shape with an initial quasi-exponential rise with $\tau_{rise} \sim$ 25000 s followed by an abrupt decline in $\sim$ 5000 s. The total duration of the hard X-ray *spike* is about half a day. The source $3 - 20$ keV flux rises by ~ 5 times from the quiescent level to the *spike* maximum and then drops by a factor of ~ 18 during the decline (Fig. 5, *left panel*). According to the AAVSO data, the optical outburst starts ~ 1 day prior to the hard X-ray *spike* (Wheatley et al. 2000), while the UV rise is coincident with sharp decline in hard X-rays.

The hard X-ray recovery at the end of an outburst has a consistent pattern from one outburst to another (Fig. 5). An exponential fit to the optical decline and X-ray rise is shown in Table 2. The X-rays appear to evolve almost twice as quickly as the optical light.

4.2. Energy spectra

Previous X-ray studies of SS Cygni (Swank 1979; Córdova et al. 1980; Jones & Watson 1992; Yoshida et al. 1992) have demonstrated the presence of two distinct spectral components: a hard component with a cut-off at $\sim 10 - 20$ keV (bremsstrahlung model), and an ultrasoft optically thick component that is cut-off at ~ 60 eV. These components behave very differently during optical outburst and quiescence. The energy range of the PCA detector allows the direct study of the hard spectral component without contamination from an ultrasoft component. The ultrasoft component is invisible to the ASM, also.

The *RXTE*/PCA spectral data were approximated with one of the simplest models that fit the data: a two-component XSPEC (version 11) model that includes an absorbed bremsstrahlung emission model and a Gaussian emission line at ~ 6.7 keV. Line emission from the source can be present at 6.4, 6.7 and/or 6.9 keV, however the energy resolution of the PCA is not sensitive enough to be able to distinguish between these lines, and we are most likely seeing a blend. While this two-component model is unphysical, it allows us to to compare our spectral results directly with previously published results. The width of the Gaussian line was fixed at 0.1 keV due to the limited energy resolution of PCA detector (~ 1 keV at 6 keV), while the line centroid energy was left as a free parameter. Typical energy spectra of SS Cygni corresponding to the optical quiescence (*upper histogram*) and outburst (*lower histogram*) are shown in Fig. 7.

The combination of an absorbed bremsstrahlung radiation model and a Gaussian emission line at ~ 6.7 keV provides a satisfactory description for the PCA spectral data in the $3 - 20$ keV energy band (Fig. 7). The best-fit value of the characteristic temperature,

kT_{bremss}, of the bremsstrahlung model varies between ~ 6 and ~ 26 keV, and the resulting model $3-20$ keV energy flux changes from $\sim 10^{11}$ to $\sim 7\times10^{-10}$ ergs s^{-1} cm^{-2}. The evolution of best-fit spectral parameters (X-ray flux and kT_{bremss}) during the 1996, 1999 and 2000 *RXTE*/PCA observations is shown in Fig. 5 (*middle* and *lower* panels). There is a unique correlation between both the hard X-ray flux and hardness of the X-ray spectrum, and the optical flux level. The X-ray flux is high and the X-ray spectrum is hard during optical quiescence, and at short periods at the beginning and the end of optical outburst. On the other hand, during the maximum of optical outburst the X-ray flux is extremely low and the X-ray spectrum is soft (corresponding to the lowest level of cut-off energy). The relative strength of the 6.7 keV emission line also is correlated with optical flux: the equivalent width of the emission line rises from ~ 350 eV during optical quiescence to ~ 800 eV during the maximum of the optical outburst.

The relation between the level of X-ray flux and the best-fit value of kT_{bremss} (hardness-intensity diagram) is shown in Fig. 8. Each point represents the data averaged over one individual observation. Fig. 8 clearly shows that the observations can be subdivided into three distinct regions according to their positions on the hardness-intensity diagram, illustrating the correlation between X-ray and optical evolution.

The first, densely populated region is concentrated around a temperature of ~ 20 keV and an X-ray flux of $\sim 2\times10^{-10}$ ergs s^{-1} cm^{-2}. This region corresponds to the periods of optical quiescence, with a relatively high level of hard X-ray flux (Fig. 5). The second, densely populated region is concentrated around a temperature of ~ 8 keV and an X-ray flux of $\sim 3\times10^{-11}$ ergs s^{-1} cm^{-2}. This group represents the periods of optical/soft X-ray outburst, characterized by an extremely low level of hard X-ray flux (Fig. 5). The third, sparsely populated group comes mostly from periods of transition between the optical outburst and quiescence, characterized by the rise of hard X-ray luminosity and general hardening of X-ray spectrum (Fig. 5). A small fraction of the observations from the third group correspond to the fast transitions from optical quiescence to the outburst.

5. DISCUSSION

It is generally believed that outbursts in DN are caused by a sudden brightening of the optically thick accretion disk due to an increased accretion rate (see Osaki 1996 for review). Two models were proposed to account for the intermittent accretion, the mass-transfer instability model (MTI; Bath 1973) and the disk instability model (DIM; Osaki 1974). It is now generally accepted that the DIM is a strong factor for DN outbursts (Osaki 1996). In the DIM the secondary star's mass transfer rate is continuous, but during

quiescence the mass flow from the secondary is not fully accreted onto the white dwarf but is mostly held up in the outer parts of the accretion disk. Once the stored mass reaches a critical amount, a thermal instability (Meyer & Meyer-Hofmeister 1981) within the disk causes this matter to flow through the disk and onto the white dwarf, resulting in optical and UV/soft X-ray outburst.

The general pattern of dwarf novae optical and X-ray behavior during outburst is traditionally explained in the framework of the DIM (Lasota 2001). Two observed features, however, appear to pose significant problems for the simple single component disk models (Meyer & Meyer-Hofmeister 1994) which are unable to reproduce: i) a sizable lag in rise-time of the UV light with respect to optical and hard X-rays rise at the beginning of the outburst and ii) the appearance and gradual decline of hard X-rays and UV light when the system falls back into quiescence.

The observed optical/hard X-ray/UV delay and the post-outburst evolution of the dwarf novae can be explained by considering models in which the inner edge of the accretion disk does not extend down to the surface of the white dwarf. Truncation of the disk can be due to evaporation of the inner part of the accretion disk (Meyer & Meyer-Hofmeister 1994), magnetic fields (e.g. Livio & Pringle 1992), or to an advection-dominated accretion flow (ADAF; Menou 2001). Here we examine the observed multiwavelength behavior of SS Cygni in the framework of the first model, evaporation of the inner disk. Let us assume that the quiescent accretion flow in SS Cygni consists of an outer optically thick cool disk truncated by evaporation at a certain radius and, inside that, an optically thin quasi-spherical boundary layer/corona structure extending down to the surface of the white dwarf.

The relative timing of the optical, hard X-ray, and soft X-ray/UV components in an SS Cygni outburst are now well established (Wheatley et al. 2003). We suggest that this sequence is an important clue for understanding the movement of material through the disk. To summarize the outburst phenomenology, after the initial optical decline, there is a short delay (~ 0.5 days) before the flaring of the hard X-ray component and an additional ~ 1 day delay before the flare in the soft X-ray and UV bands (Swank 1979; Wheatley et al. 2000; Wheatley et al. 2003). The key features of the hard X-ray flare are the fast quasi-exponential rise of the flux ($\tau_{rise} \sim 25000$ s) and an abrupt decline (Fig. 6) coincident with the rise of the UV flux (Wheatley et al. 2000).

These delays are conventionally interpreted as that passage of a heating wave through the accretion disk (Wheatley et al. 2003 and references therein). The wave starts in the outer part of the disk, causing the optical rise, then reaches the innermost region, where it initiates an increase in the mass flow from the inner edge of the disk to the boundary layer and white dwarf. This gradual increase in flow first yields an increase in the optically thin,

hard X-ray emission; at a certain critical point, the flow switches its mode into an optically thick, soft X-ray emitting plasma.

We propose an alternative explanation for the optical/hard X-ray/ soft X-ray sequence, inspired by the fact that the optical/hard X-ray delay is comparable to the dynamical timescale to fall in from the outer region of the accretion disk. In our picture, when the outburst starts, the outer disk transitions from a cool to a hot state. The increased mass accretion rate gives rise to the optical flare. The increase of this mass transfer rate, either in the outer part of the accretion disk, or in the vicinity of the inner Lagrangian point, somehow leads to an increase of the mass flow through the optically thin inner region of the accretion flow on a dynamical timescale that is comparable to the orbital period of the SS Cygni system. This requires a path for the accreting material that bypasses diffusive flow through the disk, perhaps via the sub-Keplerian flow above the disk. Once this material arrives at the inner region, it causes the initial fast rise of the hard X-ray flux (Fig. 6). The accretion rate through the optically thick accretion disk increases on a diffusive timescale, causing the rise of UV and soft X-ray flux. At some point, the rise of the UV/soft X-ray flux, combined with the increase of the accretion rate through the optically thin region, will lead to its catastrophic cooling and an abrupt softening of X-ray spectrum and abrupt drop of hard X-ray flux, as seen in the *RXTE* light curve (Fig. 6).

In this alternative picture, the optically thick disk/boundary layer will extend down to the white dwarf surface when the outburst is at maximum, and radiation driven disk winds will probably strip the coronal layers from the disk (Meyer & Meyer-Hofmeister 1994). The decline of the accretion rate during late stages of the outburst allows disk evaporation to resume, restoring the optically thin disk corona. As the corona returns, the hard X-ray flux recovers and the X-ray spectrum hardens. At the end of the optical outburst we expect that the hard X-ray flux should decay more slowly than the optical, as we observe, because the variation in $\dot{M}$ will be "smeared out" as it travels through the disk (Bath & Pringle 1981; Jones & Watson 1992). The hot/cool transition seen directly in the optical is thereby delayed and spread out as it reaches the innermost disk.

This picture also explains the phenomenon of short hard X-ray spikes associated with optical anomalous outbursts. The short-term increase of the mass transfer rate in the outer optically thick disk or in the vicinity of the inner Lagrangian point creates an increase of the mass flow in the inner optically thin region, by the same bypass that takes place in a normal outburst, and causes an increase in the hard X-ray flux. However, the smaller short spikes decays as the small mass spike is accreted, rather than being quenched by the optically thick flow through the diffusive disk as in a normal outburst.

The series of pointed *RXTE*/PCA observations allow us to trace the evolution of the

X-ray spectrum of SS Cygni in unprecedented detail. The results of spectral analysis of *RXTE*/PCA observations of SS Cygni provide additional support for the two-component model of the accretion flow mentioned above. The hard X-ray emission from non-magnetic CVs can be interpreted as due to: i) optically thin radiation from strong shocks formed in the boundary layer when the mass transfer rate was low; ii) an X-ray emitting corona-like structure above the plane of the disk/boundary layer (Meyer & Meyer-Hofmeister 1994; Frank, King & Raine 2002). In quiescence and at low disk accretion rates, the optically thin boundary layer gas is likely to be thermally unstable to turbulent viscous heating, rapidly achieving hard X-ray temperatures ($\sim 10^8$ K). At the same time, this gas is likely to expand out of the disk and boundary layer, and form a hot corona-like structure around most of the white dwarf. At quiescence (low $\dot{M}$) SS Cygni shows relatively bright, highly variable hard X-ray emission (see Wheatley et al. 2003). The energy spectrum of the source is extremely hard with a cut-off at $\sim 20 - 25$ keV (corresponding to the "QUIESCENCE" and upper parts of the "TRANSITION" region in Fig. 8) indicating the temperature of the optically thin emitting gas is $\gg 10^7$ K. At high disk accretion rates (the maximum of the optical outburst) the instability will be largely suppressed, and the boundary layer luminosity mostly emitted as soft X-rays, while the corona-like structure will be completely cooled down by rising flux of soft photons from the disk/boundary layer. After this stage we can expect the radiation driven winds to remove the coronal layer, and the hard X-rays observed during optical outburst will originate from shocks connected with such winds (Lucy & Solomon 1970; Mauche & Raymond 1987). The X-ray spectrum of SS Cygni during the optical outburst is much softer than in quiescence, with a cut-off energy of $\sim 6 - 8$ keV (Fig. 5, 8). The abrupt softening of the X-ray spectrum observed with *RXTE*/PCA at the end of the hard X-ray spikes (Fig. 5, 6) also supports the above interpretation. The recovery of the hard X-ray flux during the decline of the optical outburst is accompanied by gradual hardening of the source energy spectrum (Fig. 5, 8 (the "TRANSITION" region)), as expected from the recovery of the inner hot optically thin region. The subsequent decline of the optical and hard X-ray luminosity can be attributed to the further decrease of the mass accretion flow through the optically thick and thin regions of the accretion disk.

Our analysis of the *RXTE*/ASM and AAVSO observations of SS Cygni over a period of 6 years confirms the general picture of hard X-ray evolution deduced from more sensitive pointed observations of a handful of individual outbursts (Swank 1979; Córdova et al. 1980; Jones & Watson 1992; Yoshida et al. 1992; Wheatley et al. 2000; Wheatley et al. 2003). The average ASM light curves of SS Cygni obtained by stacking a large number of individual outbursts still show the suppression of the hard ($3 - 12.2$ keV) X-rays during both wide and narrow optical outbursts (Fig. 2).

The *RXTE*/ASM observations of SS Cygni during quiescence show some evidence for a

decrease in the hard X-ray flux during the inter-outburst periods. The observations of the post-outburst evolution of other dwarf novae often show a decrease of the optical and UV flux between outbursts (Smak 2000). The observed decrease in the X-ray, UV and optical poses additional problems for the simple DIM models, which imply a gradual increase of the luminosity (in all bands) during quiescence. On the other hand, the two-component model of the accretion flow involving disk evaporation (Meyer & Meyer-Hofmeister 1994) naturally solves this problem. As the outburst approaches its end, the inner edge of the optically thick accretion disk progressively moves outwards with time. The accretion through the coronal flow thereby decreases, causing a decline in the hard X-ray flux (Meyer & Meyer-Hofmeister 1994). This decrease in X-rays reduces the level of X-ray flux illuminating the outer parts of the accretion disk. Hence, less X-rays are reprocessed which leads to a decrease in the optical flux.

6. CONCLUSIONS

We have analyzed the variability and spectral evolution of the prototype dwarf nova system SS Cygni using simultaneous *RXTE* data (hard X-rays) and AAVSO (optical) observations. The series of pointed *RXTE*/PCA observations allow us to trace the evolution of the X-ray properties of SS Cygni in unprecedented detail. We find that our results are in general agreement with predictions of modified disk instability models that imply a two-component accretion flow, formed through the evaporation of the inner part of the optically thick accretion disk (Meyer & Meyer-Hofmeister 1994) or other process. We find that the optical and X-ray outburst morphology of SS Cygni predicted by the modified DIM and observed in a series of pointed observations is confirmed by stacking the marginal detections of individual outbursts from *RXTE*/ASM observations. The averaged light curves for the wide and narrow outbursts display a suppression of the hard ($3-12.2$ keV) X-ray flux during optical outbursts.

Based on the hard X-ray (*RXTE*/PCA/ASM) data and optical (AAVSO) observations, we quantify the time lags between the optical and X-ray outbursts, and the time scales of the X-ray spectral recovery from outburst. We also find that anomalous optical outbursts of SS Cygni are accompanied by short hard X-ray outbursts lasting $\sim 1-2$ days.

Using the *RXTE*/ASM data, we find evidence for a decrease in the hard X-ray flux during quiescence. While this is in disagreement with a simple DIM which predicts an increase in the disk mass, constant or decreasing flux has been observed in optical and UV studies of other dwarf novae (e.g. Smak 2000). It should be mentioned that a modified DIM involving a two-component accretion flow (Meyer & Meyer-Hofmeister 1994) naturally

solves this problem, by predicting the decrease of hard X-ray and optical/UV flux due to the outward motion of the inner boundary of optically thick accretion disk due to its evaporation into a corona-like structure.

We folded the quiescent $1.3 - 12.2$ keV X-ray data on the orbital period, but do not find any significant modulation. An all-sky monitor a few times more sensitive than the *RXTE*/ASM would allow us to study individual outbursts and the quiescent behavior of SS Cygni with much greater signal to noise, and to extend these studies to a large number of dwarf nova (Priedhorsky, Peele & Nugent 1996).

7. ACKNOWLEDGMENTS

We thank Peter Wheatley for useful discussions. This research has made use of data obtained through the High Energy Astrophysics Science Archive Research Center Online Service, provided by the NASA/Goddard Space Flight Center. In this research, we have used, and acknowledge with thanks, data from the AAVSO International Database, based on observations submitted to the AAVSO by variable star observers worldwide.

REFERENCES

Bath, G.T., 1973, NPhS, 246, 84

Bath, G.T., Pringle, J.E., 1981, MNRAS, 194, 967

Bradt, H.V., Rothschild, R.E., Swank, J.H., 1993, A&AS, 97, 355

Córdova, F.A., Chester, T.J., Tuohy, I.R., Garmire, G.P., 1980, ApJ, 235, 163

Córdova, F.A., Chester, T.J., Mason, K.O., Kahn, S.M., Garmire, G.P., 1984, ApJ, 278, 739

Doty, J.P., 1988, Proc. SPIE, 982, 164

Frank, J., King, A.R., Raine, D.J., 2002, Accretion Power in Astrophysics, Cambridge University Press, Cambridge

Friend, M.T., Martin, J.S., Smith, R.C., Jones, D.H.P., 1990, MNRAS, 246, 654

Jahoda, K., et al., 1996, Proc. SPIE, 2808, 59

Jones, M.H., Watson, M.G., 1992, MNRAS, 257, 633

Lasota, J.-P., 2001, NewAR, 45, 449

Levine, A.M., et al., 1996, ApJ, 469 L33

Livio, M., Pringle, J.E., 1992, MNRAS, 259, 23

Lucy, L. B., Solomon, P., 1970, ApJ, 159, 878

Mauche, C. W., Raymond, J. C., 1987, ApJ, 323, 690

McGowan, K., Priedhorsky, W., Trudolyubov, S., 2002, Proc. of "X-ray Binaries in the Chandra and XMM-Newton Era (with emphasis on Targets of Opportunity)", MIT Draper Labs Extension, Cambridge MA

Menou, K., 2001, ApJ, submitted (astro-ph/0007185)

Meyer, F., Meyer-Hofmeister, E., 1981, A&A, 104, 10

Meyer, F., Meyer-Hofmeister, E., 1994, A&A, 288, 175

Osaki, Y., 1974, PASJ, 26, 429

Osaki, Y., 1996, PASP, 108, 39

Priedhorsky, W.C., Peele, A.G., Nugent, K.A., 1996, MNRAS, 279, 733

Priedhorsky, W., Trudolyubov, S., McGowan, K., 2002, Joint American Physical Society and High Energy Astrophysics Division Meeting, APR02, X11.006

Pringle, J.E., Savonije, G.J., 1979, MNRAS, 187, 777

Rappaport, S., Cash, W., Doxsey, R., McClintock, J., Moore, G., 1974, ApJ, 187, L5

Ricketts, M.J., King, A.R., Raine, D.J., 1979, MNRAS, 186, 233

Smak, J., 2000, NewAR, 44, 171

Swank, J.H., 1979, White Dwarfs and Variable Degenerate Stars, IAU Colloq. No. 53, 135, eds van Horn, H.M., Weidemann, V., Rochester University Press, Rochester

Szkody, P., Mattei, J.A., 1984, PASP, 96, 988

Wheatley, P.J., Mauche, C.W., Mattei, J.A., 2000, NewAR, 44, 33

Wheatley, P.J., Mauche, C.W., Mattei, J.A., 2003, MNRAS, 345, 49

Yoshida, K., Inoue, H., Osaki, Y., 1992, PASJ, 44, 537

Table 1: Pointed *RXTE*/PCA observations of SS Cygni used in this analysis.

Proposal ID	Year	Start Date – End Date	No. of observations	Total exp. time (ks)
P10040	1996	Oct. 9 – Oct. 21	25	500
P20033	1997	Mar. 1 – Jul. 2	42	190
P40012	1999	Jun. 7 – Jun. 21	20	70
P50011	2000	Mar. 5 – Jun. 3	185	147

Table 2: Parameters of an exponential approximation for the rising phase in the $3-20$ keV energy band (*RXTE*/PCA data) and decline in the optical band (AAVSO data).

Observational interval MJD	Year	$\tau_{\rm X-ray}$ d	τ_{opt} d
$50373-50378$	1996	0.73 ± 0.20	2.00 ± 0.02
$51336-51350$	1999	1.15 ± 0.15	2.40 ± 0.02
$51627-51643$	2000	1.42 ± 0.10	2.45 ± 0.02
$51681-51691$	2000	1.40 ± 0.10	2.30 ± 0.02

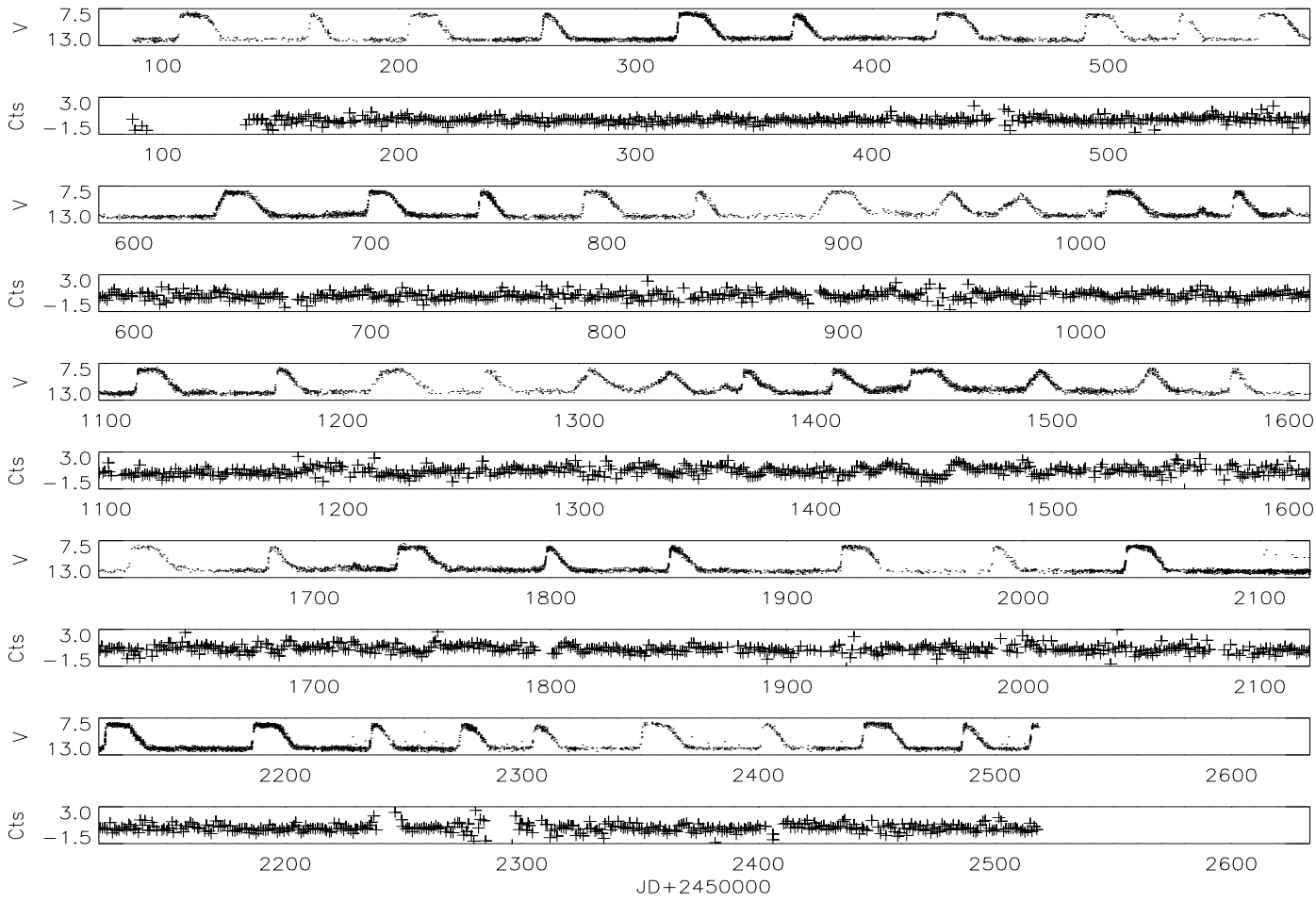

Fig. 1.— Contemporaneous optical (panels 1, 3, 5, 7 and 9) and X-ray (panels 2, 4, 6, 8 and 10) light curves of SS Cygni from 1996 January 4 to 2001 August 30. The optical data is from the AAVSO, the X-ray data is from *RXTE*/ASM. The X-ray data are binned in one day intervals.

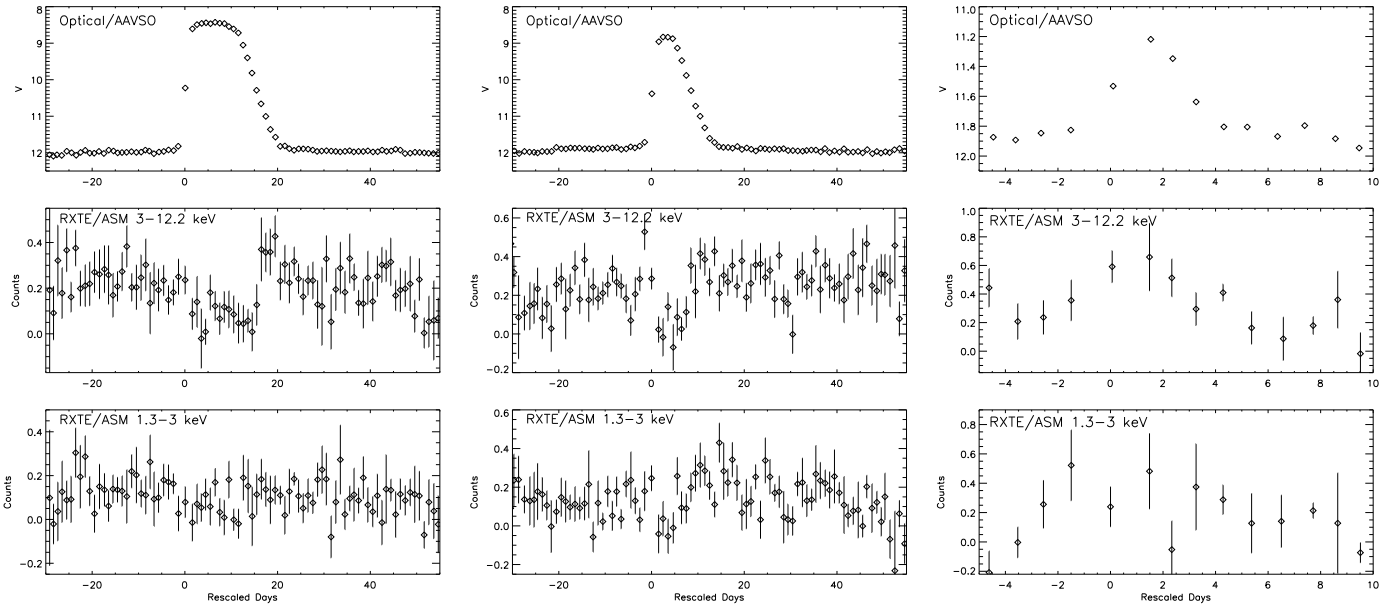

Fig. 2.— Averaged outburst data of SS Cygni produced using a stacking technique (see text). Data shown are for wide (*left*), narrow (*middle*) and anomalous (*right*) outbursts. In each case, the optical data is plotted in the *top* panel, the $3 - 12.2$ and $1.3 - 3$ keV X-ray data from the *RXTE*/ASM are plotted in the *second* and *third* panels, respectively.

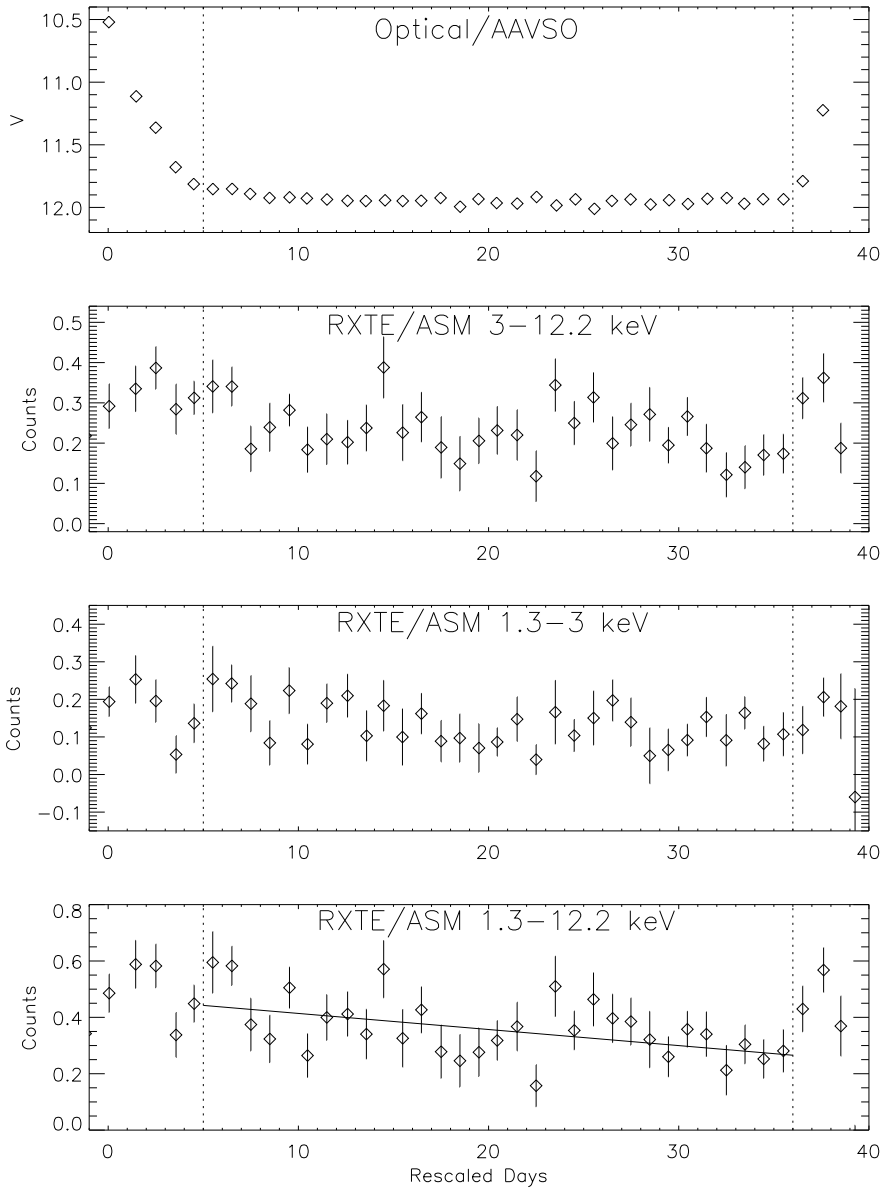

Fig. 3.— Averaged data for the inter-outbursts. *First* panel, optical AAVSO data. *Second* and *third* panels, 3−12.2 and 1.3−3 keV ASM data, respectively. Fourth panel, 1.3−12.2 keV ASM X-ray flux. The *dotted* lines indicate the start and end points of quiescence. The *solid* line shows the best-fit decline to the data.

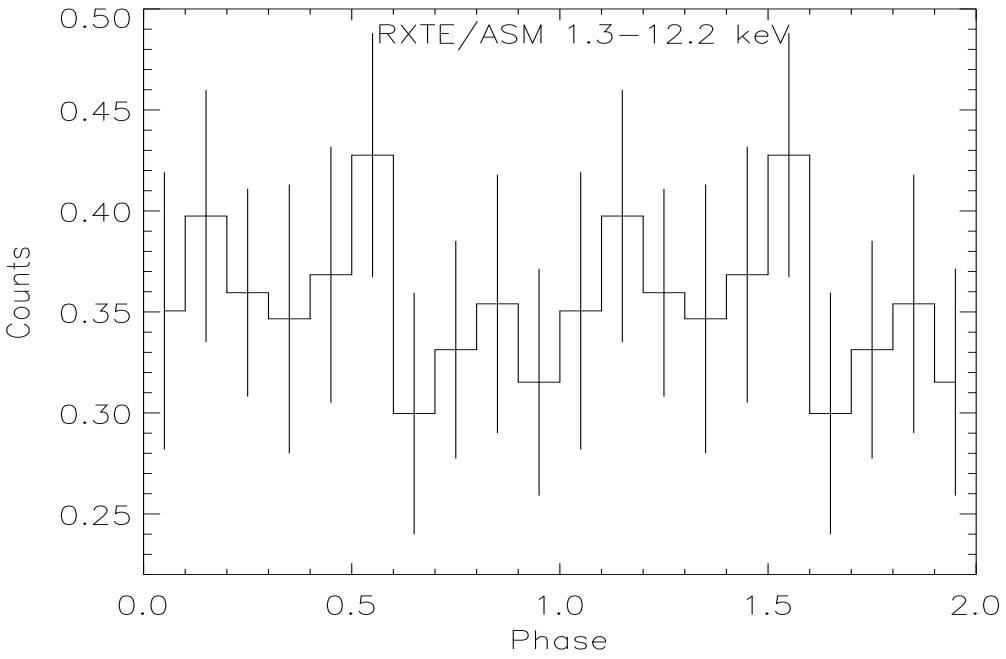

Fig. 4.— Quiescent *RXTE*/ASM data in the 1.3−12.2 keV range folded on $P_{orb} = 0.2751297$ d with T_0 = HJD 2447403.6295.

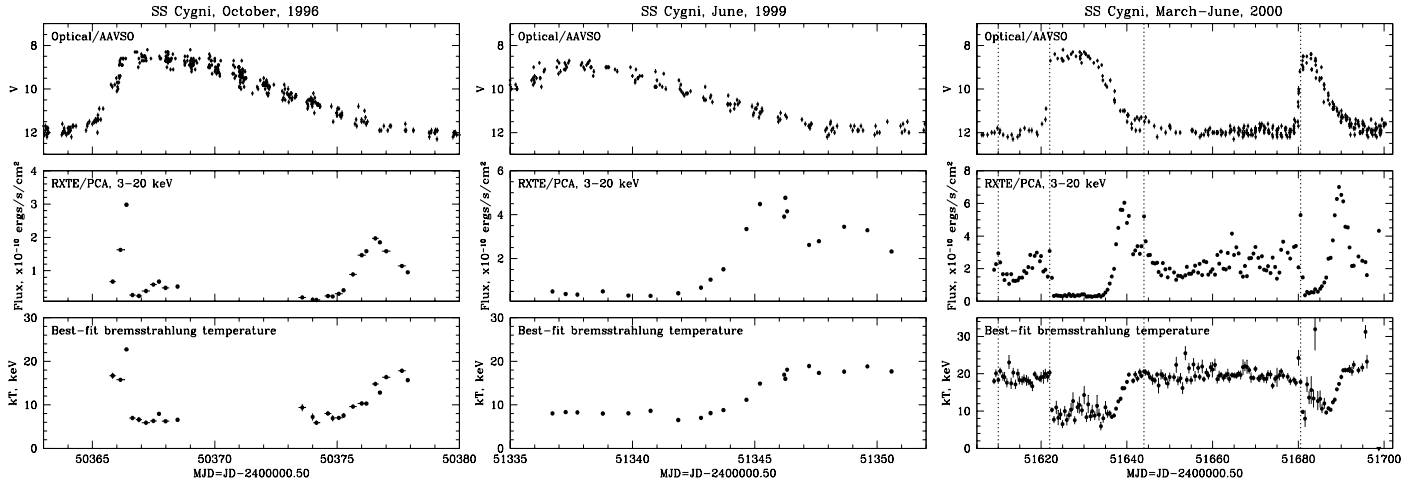

Fig. 5.— Simultaneous optical (AAVSO) and X-ray (*RXTE*/PCA) evolution of SS Cygni in October, 1996 (*left*), June, 1999 (*middle*) and between March and June, 2000 (*right*). The X-ray data points represent the average of each of the individual PCA observations which had exposure times ranging from $\sim 1000 - 20000$ s. The evolution of the optical and X-ray flux are shown in the *upper* and *middle* panels. The *lower* panel shows the evolution of the hardness of the X-ray spectrum expressed in terms of the best-fit bremsstrahlung temperature. Vertical *dotted* lines mark the positions of X-ray *spikes*.

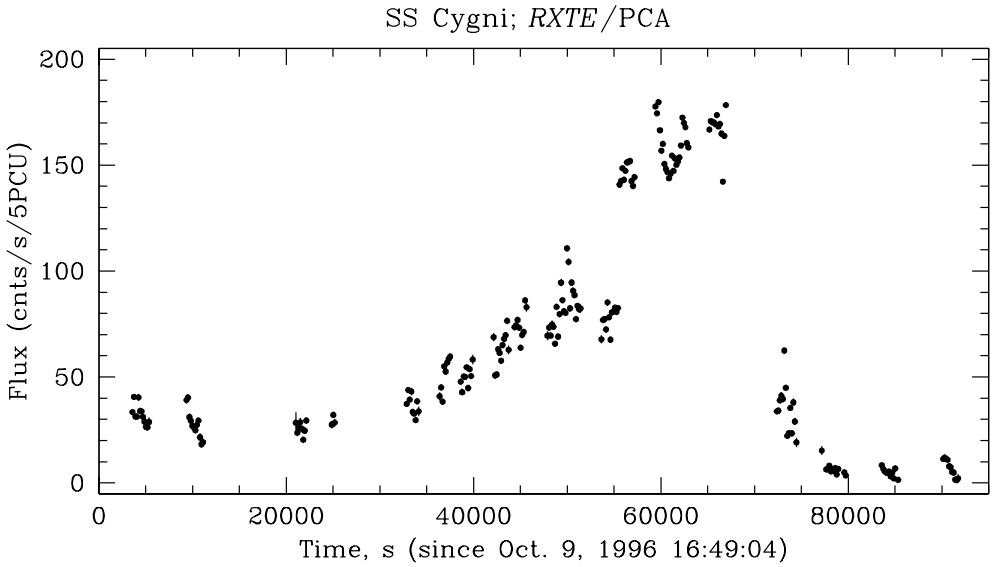

Fig. 6.— A detailed evolution of the X-ray flux from SS Cygni during the X-ray *spike* on Oct. 9 – 10, 1996 (MJD $\sim$ 50366, see also *left panel* in Fig. 5). *RXTE*/PCA data, $3 - 20$ keV energy range.

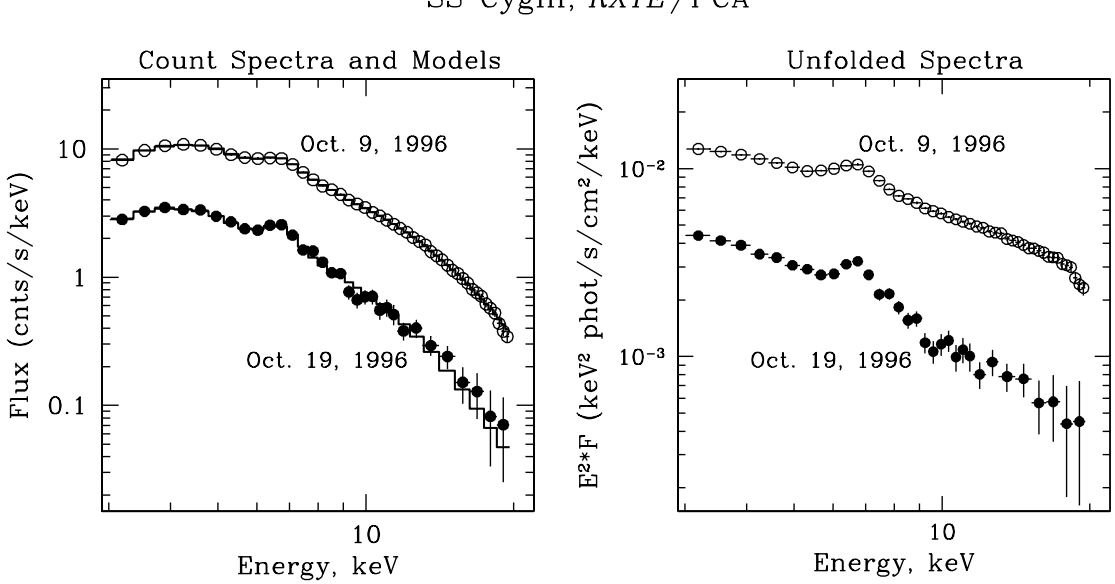

Fig. 7.— Representative count (*left panel*) and corresponding unfolded (*right panel*) spectra of SS Cygni in the high (Oct. 9, 1996) and low-flux (Oct. 19, 1996) states. PCA data, $3 - 20$ keV energy range. The best-fit analytical models (sum of bremsstrahlung spectrum and Gaussian emission line) are shown as histograms in the *left panel*.

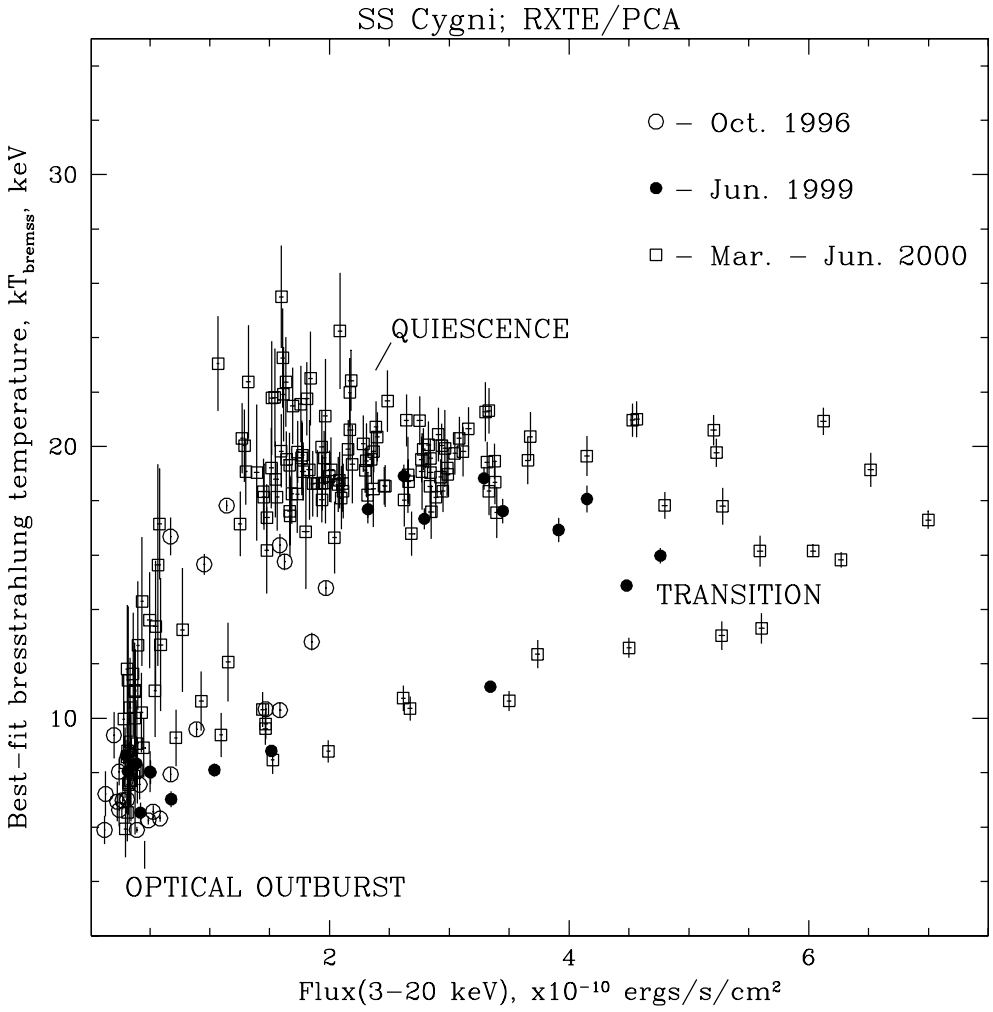

Fig. 8.— Hardness of the X-ray spectrum in terms of best-fit bremsstrahlung temperature vs. total X-ray flux in the $3-20$ keV energy range. The *open* and *filled* circles represent 1996, October and 1999, June data, *open* squares correspond to March-June, 2000 observations.